Article

Discovery Medicine 2024; 36(181): 343–354
https://doi.org/10.24976/Discov.Med.202436181.32

Foam Cell Targeted Liposomes Co-Encapsulating Superoxide Dismutase and Catalase to Attenuate Atherosclerosis by Inhibiting Oxidative Stress

Shuang Zhang[1,2,3], Danni Liu[1,2,3], Jie Zhang[1,2,3], Siyu Liu[1,2,3], Ran Sun[1,2,3], Ran Huo[1,2,3], Chunying Cui[1,2,3,*]

[1]School of Pharmaceutical Sciences, Capital Medical University, 10069 Beijing, China
[2]Engineering Research Center of Endogenous Prophylactic of Ministry of Education of China, 10069 Beijing, China
[3]Beijing Area Major Laboratory of Peptide and Small Molecular Drugs, 10069 Beijing, China
*Correspondence: ccy@ccmu.edu.cn (Chunying Cui)
Published: 20 February 2024

Background: Oxidative stress, propelled by reactive oxygen species (ROS), serves as a significant catalyst for atherosclerosis (AS), a primary contributor to vascular diseases on a global scale. Antioxidant therapy via nanomedicine has emerged as a pivotal approach in AS treatment. Nonetheless, challenges such as inadequate targeting, subpar biocompatibility, and limited antioxidant effectiveness have restrained the widespread utilization of nanomedicines in AS treatment. This study aimed to synthesize a specialized peptide-modified liposome capable of encapsulating two antioxidant enzymes, intending to enhance targeted antioxidant therapy for AS.

Methods: The film dispersion method was employed for liposome preparation. Fluorescence quantification was conducted to assess the drug encapsulation rate. Characterization of liposome particle size was performed using dynamic light scattering (DLS) and transmission electron microscopy (TEM). Laser confocal microscopy and flow cytometry were utilized to analyze liposome cell uptake and target foam cells. Antioxidant analysis was conducted using 2′,7′-Dichlorodihydrofluorescein diacetate (DCFH-DA) staining, while pro-lipid efflux analysis utilized Oil Red O (ORO) staining. Safety evaluation was performed using Hematoxylin and Eosin (H&E) staining. The level of inflammatory factors was determined through enzyme-linked immunosorbent assay (ELISA). The degree of lipid oxidation at the cellular level was assessed using the malonaldehyde (MDA) assay. *In vivo* targeting analysis was conducted using small animal live imaging.

Results: Our *in vitro* and *in vivo* findings substantiated that the modification of Lyp-1 led to increased delivery of antioxidant enzymes into foam cells ($p < 0.05$), the primary pathological cells within AS plaques. Upon accumulation in foam cells, liposomes loaded with superoxide dismutase (SOD) and catalase (CAT) (LyP-lip@SOD/CAT) effectively mitigated excess ROS and shielded macrophages from ROS-induced damage ($p < 0.01$). Furthermore, the reduction in ROS levels notably hindered the endocytosis of oxidized low-density lipoprotein (Ox-LDL) by activated macrophages, subsequently alleviating lipid accumulation at atherosclerotic lesion sites, evident from both *in vitro* and *in vivo* ORO staining results ($p < 0.01$). LyP-lip@SOD/CAT significantly curbed the secretion of inflammatory factors at the plaque site ($p < 0.001$). Additionally, LyP-lip@SOD/CAT demonstrated commendable biological safety.

Conclusions: In this study, we effectively synthesized LyP-lip@SOD/CAT and established its efficacy as a straightforward and promising nano-agent for antioxidant therapy targeting atherosclerosis.

Keywords: antioxidant; liposome; SOD/CAT; LyP-1; atherosclerosis

Introduction

Cardiovascular disease (CVD) continues to be the primary cause of both morbidity and mortality worldwide [1]. Atherosclerosis (AS) stands as the principal factor contributing to CVDs. AS represents a chronic arterial condition stemming from lipid metabolism irregularities, primarily affecting medium and large arteries. It stands as the most prevalent underlying cause of conditions such as coronary heart disease, carotid artery disease, and peripheral arterial disease [2].

Oxidative stress plays a significant role in the progression of atherosclerotic disease. During the early stages of atherogenesis, reactive oxygen species (ROS) oxidize low-density lipoproteins, leading to the transformation of macrophages into foam cells. Additionally, ROS can disrupt redox-dependent signaling in the vascular wall, thereby fostering the advancement of atherosclerosis [3]. Extensive experimentation has confirmed that mitigating oxidative stress serves as a rational approach in the treatment of atherosclerosis [4].

Antioxidants like N-acetylcysteine have been employed in treating AS [5], effectively countering oxidative damage by intercepting free radicals before they inflict harm on intracellular biomolecules [6]. Among various antioxidants, endogenous antioxidant enzymes such as superoxide dismutase (SOD) and catalase (CAT) play pivotal roles in eliminating endogenous ROS [7]. SOD stands as the sole enzyme capable of eliminating the superoxide anion radical, sparking therapeutic interest since its discovery in 1969 [8]. Nevertheless, SOD's catalytic substrate, hydrogen peroxide (H_2O_2), may prompt cellular damage [9]. Conversely, CAT can convert H_2O_2 into harmless water (H_2O) [10], making the combination of SOD and CAT an optimal strategy to neutralize the oxidative stress milieu within cells.

While the use of antioxidants for AS treatment has garnered significant attention, clinical benefits in most AS patients have been limited. Findings from animal and clinical studies indicate that direct administration of free antioxidant enzymes offers only modest protection against oxidative damage due to inherent characteristics of these enzymes, including inadequate retention at the disease site and rapid inactivation [11]. Consequently, the development of an effective delivery system to enhance the accumulation of SOD and CAT within atherosclerotic plaques, while safeguarding against degradation during *in vivo* delivery, becomes imperative for their successful application in treating atherosclerosis.

Nanoparticles (NPs) have emerged as a promising and effective vehicle for molecular imaging and therapy in atherosclerosis [12]. These particles can directly access plaques by penetrating damaged or dysfunctional endothelial barriers, facilitating targeted therapy [13]. Among nanoparticle types, liposomes (Lip) are spherical vesicle systems composed of lipids, capable of carrying both hydrophilic and hydrophobic drugs. Liposomes have been successfully employed in delivering genes, stem cells, as well as anti-inflammatory or anti-angiogenic drugs to atherosclerotic plaque sites [14]. They can electrostatically adhere to negatively charged cell membranes, facilitating cellular uptake, making them suitable for *in vitro* and *in vivo* protein delivery [15].

Additionally, liposomes exhibit efficient escape from endosomes due to their ability to disrupt endosomal membranes and utilize the proton sponge effect, enabling protein delivery into the cytoplasm [16]. Therefore, liposomes stand as an ideal carrier for delivering SOD and CAT for antioxidant therapy in AS. In the realm of nano-delivery systems, a common challenge for atherosclerosis treatment and diagnosis is the lack of precise targeted delivery to plaques. LyP-1 (CGNKRTRGC) is a cyclic peptide that specifically binds to its receptor, p32 protein, which is overexpressed in various tumor-associated cells and macrophages present in atherosclerotic plaques. Over recent years, several LyP-1-based nano-delivery systems have been designed and developed for clinical diagnostic and therapeutic purposes [17].

Research indicates that LyP-1 exhibits exceptional specificity for atherosclerotic plaques, effectively penetrating these plaques and accumulating in plaque macrophages without significant side effects [18]. In comparison to non-modified liposomes, LyP-1 liposomes were notably absorbed by foam cells *in vitro* and demonstrated higher accumulation at atherosclerotic plaques *in vivo* [19]. Hence, selecting LyP-1 as a peptide ligand for modifying liposomes and targeting foam cells represents an effective strategy for precise therapy in atherosclerosis.

In this study, our aim was to devise a liposomal drug delivery system that merges the targeting capabilities of LyP-1 with the antioxidant properties of enzymes (SOD, CAT). The goal was to diminish oxidative stress levels within foam cells at atherosclerotic plaques, eliminating excessive ROS. This approach was intended to decelerate the progression of atherosclerotic plaques and potentially reverse the disease (Fig. 1). LyP-lip@SOD/CAT was designed to selectively accumulate within atherosclerotic plaques, mitigate excessive ROS to shield macrophages from ROS-induced harm, diminish the release of inflammatory factors, and execute effective antioxidant therapeutic effects.

Experimental Methods

Materials

Superoxide dismutase (R006118, RHAWN, Shanghai, China), catalase (C6319, Macklin, Shanghai, China), cholesterol (R008055, RHAWN, Shanghai, China), 1,2-dioleoyl-3-trimethylammonium propane (DOTAP, LP-R4-117, Corden Rharma Switzerland LLC, Liestal, Halbkanton, Switzerland), hydrogenated soybean phospholipids (HSPC, H902414, Macklin, Shanghai, China), DSPE-mPEG2k (D163614, Aladdin, Shanghai, China), and DSPE-mPEG2k-NHS (D163641, Aladdin, Shanghai, China) were utilized in liposome preparation. Cy3-NHS (11020, Lumiprobe, Cockeysville, MD, USA) and Cy5.5-NHS (17020, Lumiprobe, Cockeysville, MD, USA) were employed to fluorescently label SOD and CAT. The LyP-1 peptide (NJP91490, Nanjing Peptide Biological Co., Nanjing, China) was used to modify liposomes as a targeting agent. Oil Red O (O104972, Aladdin, Shanghai, China) was employed for cell and aortic staining.

Preparation and Characterization of LyP-lip@SOD/CAT

The liposomes were prepared using an enhanced thin film hydration method. SOD (0.2 mg dissolved in water) and CAT (0.4 mg dissolved in water) were combined with an equal mass of DOTAP (dissolved in chloroform), followed by the addition of an equal volume of methanol to achieve a homogeneous solution. After 30 minutes of incubation at room temperature, an equivalent volume

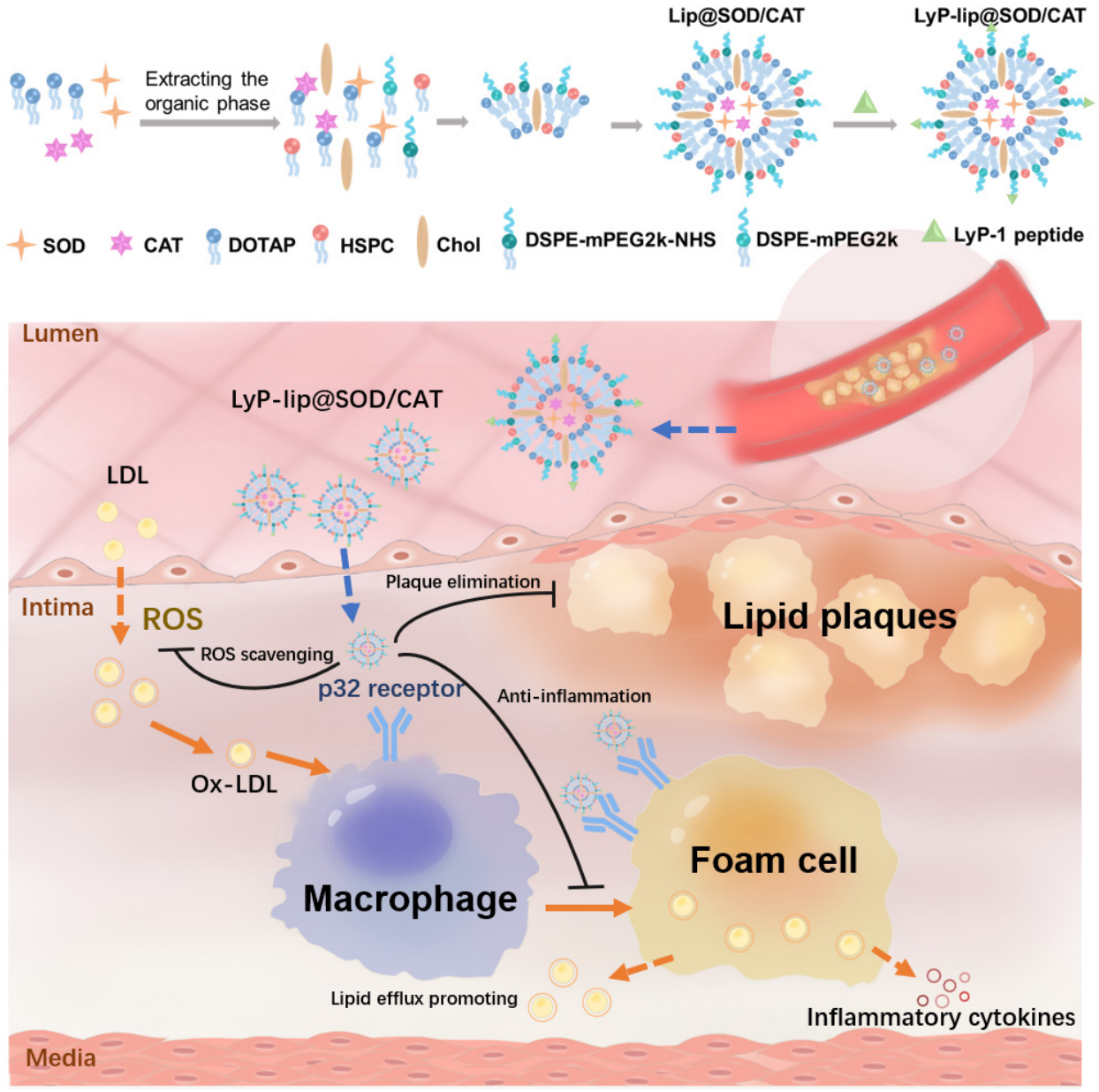

Fig. 1. Preparation of LyP-lip@SOD/CAT and its mechanism of targeting foam cells for treating atherosclerosis. After encapsulating the antioxidant enzymes SOD and CAT within liposomes, the surface of these liposomes was modified with the targeted peptide LyP-1. LyP-lip@SOD/CAT was designed to specifically adhere to the p32 receptor, which is overexpressed on foam cell surfaces. By accumulating within foam cells, it aims to impede the advancement of atherosclerosis through multiple mechanisms: scavenging excessive ROS, inhibiting LDL oxidation, diminishing the release of pro-inflammatory cytokines, and enhancing lipid efflux. This figure was created using Photoshop. SOD, superoxide dismutase; CAT, catalase; ROS, reactive oxygen species; Ox-LDL, oxidized low-density lipoprotein; DOTAP, 1,2-dioleoyl-3-trimethylammonium propane; HSPC, hydrogenated soybean phospholipids; Chol, cholesterol.

of chloroform and water was introduced to the mixture. Following centrifugation (419 ×g, 8 min), the upper organic phase was collected. This organic phase was then added to 4 mL of a lipid mixture dissolved in chloroform (HSPC: Chol: DSPE-mPEG2k: DSPE-mPEG2k-NHS = 4.24 mg:1.6 mg:0.72 mg:0.08 mg) for subsequent centrifugation. Subsequently, 4 mL of a 5% glucose solution was incorporated for hydration, followed by sonication to ensure proper dispersion. Purification and concentration of the liposomes were carried out using Amicon Ultra centrifugal filter units (MWCO-100000, Millipore Inc., Billerica, MA, USA) through centrifugation for 30 minutes at 1400 ×g (Centrifuge 5810-R, Eppendorf AG, Hamburg, Germany). For peptide conjugation, the liposomes were incubated with a LyP-1 peptide solution in phosphate buffer saline (PBS) for 30 minutes in the dark, as

described previously [20]. Removal of unconjugated peptide was accomplished using a Desalting column G25 M (20590ES03, Yeasen, Shanghai, China). The resulting LyP-lip@SOD/CAT complexes were concentrated and stored at 4 °C for future studies.

To achieve fluorescent labeling of SOD and CAT, 10 μg of fluorescent dye was combined with SOD/CAT (4 mg dissolved in water) and subjected to incubation at room temperature for 2 hours. Additionally, an overnight incubation at 4 °C was performed, followed by a 24-hour dialysis process. Subsequently, fluorescently labeled liposomes were prepared following the previously described method. Dynamic light scattering (DLS) and Zeta potential measurements were conducted using a Malvern Zetasizer (Nano Z90, Malvern, London, UK). The morphology of LyP-lip@SOD/CAT was observed using a transmission electron microscopy (TEM) (JEM-2100, Tokyo, JEOL, Japan) after staining the liposomes with phosphotungstic acid (2 wt%, pH = 7.4) in accordance with standard procedures. LyP-lip@Cy5.5-SOD/CAT and LyP-lip@SOD/Cy3-CAT were prepared as previously outlined. The binding capacity of DOTAP and SOD/CAT, as well as the encapsulation rates of SOD and CAT, were analyzed using a fluorescence spectrophotometer (RF-6000, SHIMADZU, Kyoto, Japan).

Evaluation of LyP-lip@SOD/CAT Activity

The antioxidant enzyme activity within LyP-lip@SOD/CAT was assessed by measuring the efficiency of H_2O_2 scavenging. In brief, both free SOD/CAT and LyP-lip@SOD/CAT (with a CAT concentration of 100 μg/mL) were introduced into a 0.5 mL H_2O_2 solution (50 mM) and allowed to react at 37 °C for 5 minutes. A 50 mM H_2O_2solution without any treatment served as the control. The remaining H_2O_2 was quantified using a hydrogen peroxide detection kit (TO1076, Leagene, Beijing, China). The clearance rate of H_2O_2 was calculated utilizing the following equation: Clearance rate of H_2O_2 (%) = (content of H_2O_2 with control – content of H_2O_2 with sample) / (content of H_2O_2 with control) × 100.

Cell Culture

The Raw264.7 cell line was acquired from the Cell Bank of the Chinese Academy of Medical Sciences, and was tested to be free of mycoplasma contamination. For cell culture, Dulbecco's modified eagle medium (DMEM) medium (M&C gene technology LTD, Beijing, China), fetal bovine serum (PAN-Seratech, Aidenbach, Germany), and Penicillin and Streptomycin (HyClone, Logan, UT, USA) were prepared. Raw264.7 cells were maintained in DMEM supplemented with 10% fetal bovine serum. All cell culture media were further supplemented with penicillin (100 U/mL) and streptomycin (100 μg/mL). Cultivation was carried out in a humidified 5% CO_2 incubator at 37 °C.

Evaluation of Cell Toxicity of LyP-lip@SOD/CAT

To assess the toxicity of various LyP-lip@SOD/CAT formulations, cell viability was determined using the methylthiazolyldiphenyl-tetrazolium bromide (MTT) method. RAW264.7 cells were initially seeded into 96-well plates at a density of 5×10^3 cells per well and allowed to adhere for 12 hours. Subsequently, these cells were exposed to different concentrations of LyP-lip@SOD/CAT (with a CAT dosage range of 0–200 μg/mL) for a duration of 48 hours.

Following the incubation period, 25 μL of MTT solution (5 mg/mL, Aladdin, Shanghai, China) was added to each well, and the cells were further incubated for 4 hours at 37 °C. Afterward, 150 μL of a DMSO (dimethyl sulfoxide) solution was introduced into each well and placed on a shaker for 5 minutes. The absorbance was measured at 570 nm using a microplate reader (Multiskan Spectrum 1500, Thermo, Waltham, MA, USA).

Cellular viability was calculated using the formula:

Cell viability (%) = (OD treatment group – OD blank) / (OD control group – OD blank) × 100.

Macrophages and Foam Cells Uptake of LyP-lip@SOD/CAT

To examine the uptake of different liposomes by both macrophages and foam cells, RAW264.7 cells were seeded onto a 25 mm confocal dish at a concentration of 1×10^5 cells per dish and allowed to adhere for 12 hours. For the generation of foam cells, RAW264.7 cells were treated with 25 μg/mL oxidized low-density lipoprotein (Ox-LDL, IO1300, Solarbio, Beijing, China) for 48 hours. Following this, both macrophages and foam cells were exposed to lip@SOD/CAT or LyP-lip@SOD/CAT labeled with Cy3 fluorescence for a duration of 6 hours. Subsequently, after washing the cells thrice with PBS, the cultured cells were stained with Hoechst 33342 (Life Technologies, Carlsbad, CA, USA). Observation and imaging were conducted using a laser confocal microscope (TCS SP5, Leica, Wetzlar, Germany). In addition to imaging, cellular uptake was quantified using a BD LSRFortessa Flow Cytometer (Becton, Dickinson and Company, Franklin Lakes, NJ, USA) in parallel with the imaging analysis.

Scavenging ROS and Anti-Lipid-Oxidation of the LyP-lip@SOD/CAT

RAW264.7 cells were seeded in 24-well plates at a concentration of 1×10^5 cells per well and allowed to adhere for 12 hours. Subsequently, the cells were stimulated with 20 μg/mL LPS (lipopolysaccharides, S11060, Yuanye, Shanghai, China) for a duration of 8 hours. Following this, the cells were treated with various samples (100 μg/mL CAT) for an additional 12 hours. After removing the drug-containing medium, the cells were washed with PBS, and a medium containing 10 μM 2′,7′-Dichlorodihydrofluorescein diacetate (DCFH-DA) (HY-D0940, MCE, Monmouth Junction, NJ, USA) was added

for co-incubation at 37 °C for 30 minutes. Subsequently, the fluorescently labeled cells were washed twice with PBS and examined using a fluorescence microscope (Axio vert 5, Zeiss, Jena, Germany). To assess the anti-lipid oxidation effects, cells were treated as previously described. Subsequently, the levels of lipid oxidation were measured using a malonaldehyde (MDA) assay kit (S0131S, Beyotime, Shanghai, China), while total protein levels were determined using a BCA (Bicinchoninic Acid Assay) kit (23227, Thermo, Waltham, MA, USA).

Anti-Inflammation of the LyP-lip@SOD/CAT

RAW264.7 cells were seeded into 24-well plates at a concentration of 1×10^5 cells per well and allowed to adhere for 12 hours. The negative control group received fresh medium, while the experimental groups were stimulated with 20 µg/mL LPS for 8 hours. Subsequently, cells were treated with different samples (100 µg/mL CAT) for 6 hours and further incubated for an additional 42 hours. Following this incubation period, enzyme-linked immunosorbent assay (ELISA) (PT512 for tumor necrosis factor-α (TNF-α), PI301 for interleukin-1β (IL-1β), PC125 for monocyte chemoattractant protein-1 (MCP-1), Beyotime, Shanghai, China) was utilized to assess typical inflammatory factors in the cell culture media supernatants [3], including TNF-α, IL-1β, and MCP-1. Moreover, the total protein content was determined using a BCA kit (Thermo, USA).

Inhibition of Cellular Uptake of Ox-LDL by LyP-lip@SOD/CAT

In short, RAW264.7 cells were seeded into 24-well plates at a concentration of 1×10^5 cells per well and allowed to adhere for 12 hours. The negative control group received a fresh medium, while the remaining groups were stimulated with 25 µg/mL Ox-LDL for 8 hours. Following this, cells were treated with various samples (100 µg/mL CAT) for 6 hours and then incubated for an additional 42 hours. Afterward, the cells were washed with PBS, fixed using 4% paraformaldehyde, and subsequently stained with 0.3% Oil Red O (ORO) solution (dissolved in 60% isopropanol) for 20 minutes at room temperature. The ORO stain was then washed away using PBS, and cell staining was observed under the bright field of a microscope (Ts2RFL, Nikon, Tokyo, Japan).

Animals

Animal care and experiments were conducted in line with the Guide for the Care and Use of Laboratory Animals proposed by National Institutes of Health. All procedures and protocols were approved by the Institutional Animal Ethics Committee of Capital Medical University. Apolipoprotein E-deficient ($ApoE^{-/-}$) mice, approximately 8 weeks old and weighing 20 g, were procured from the Animal Department of Capital Medical University (Beijing Laboratory Animal Center, Beijing, China). To establish the AS model, mice were fed a high-fat diet (HFD) containing 20% fat, 20% sugar, and 1.25% cholesterol for a duration of 8 weeks [21]. Subsequently, the mice were divided into four groups and received treatment via intravenous injection with the following substances: a 5% glucose solution, a mixture solution of SOD/CAT, Lip@SOD/CAT, and LyP-lip@SOD/CAT. The administration frequency of the drugs was once every four days, totaling six doses over the course of treatment. After four weeks of treatment, all mice were humanely euthanized through CO_2 gas anaesthesia followed by cervical dislocation to facilitate subsequent experiments.

Plaque Targeting and Tissue Distribution of LyP-lip@SOD/CAT in Vivo

To assess the targeting efficacy of LyP-lip@SOD/CAT in AS model mice, Cy5.5-labeled SOD/CAT was employed for animal fluorescence imaging. The model mice received treatment via intravenous injection with free Cy5.5-SOD/CAT, lip@Cy5.5-SOD/CAT, or LyP-lip@Cy5.5-SOD/CAT for each mouse. Following an 8-hour interval, the mice were placed under anesthesia and transcardially perfused with 30 mL PBS followed by 30 mL of 4% paraformaldehyde. Subsequently, the aorta and primary organs, including the heart, liver, spleen, lung, and kidney, were isolated and subjected to imaging using a fluorescence imaging system (IVIS Spectrum, Waltham, MA, USA).

Quantification of Atherosclerotic Plaques by ORO Staining

After euthanizing the AS model mice, the aorta was carefully excised, and any surrounding adipose tissue was meticulously removed. The aorta was then fixed overnight using 4% paraformaldehyde. Following this, the aorta was rinsed with PBS and longitudinally sectioned. To quantify the plaque area, the aorta sections were stained with 0.3% ORO solution (dissolved in 60% isopropanol) for 30 minutes. Subsequently, the ORO stain was washed away using 70% ethanol, allowing for clearer visualization and quantification of the plaque area in the aorta.

In Vivo Safety Evaluation

The sections of major organs were subjected to Hematoxylin and Eosin (H&E) staining. Images of the stained sections were then observed using a fluorescence microscope (Eclipse Ti-SR, Nikon, Japan).

Statistics Analysis

The data was presented as mean $\pm$ standard deviation (SD). Statistical analysis was conducted using the *t*-test. A value of $p < 0.05$ was deemed statistically significant, while $p < 0.01$ or $p < 0.001$ was considered highly significant.

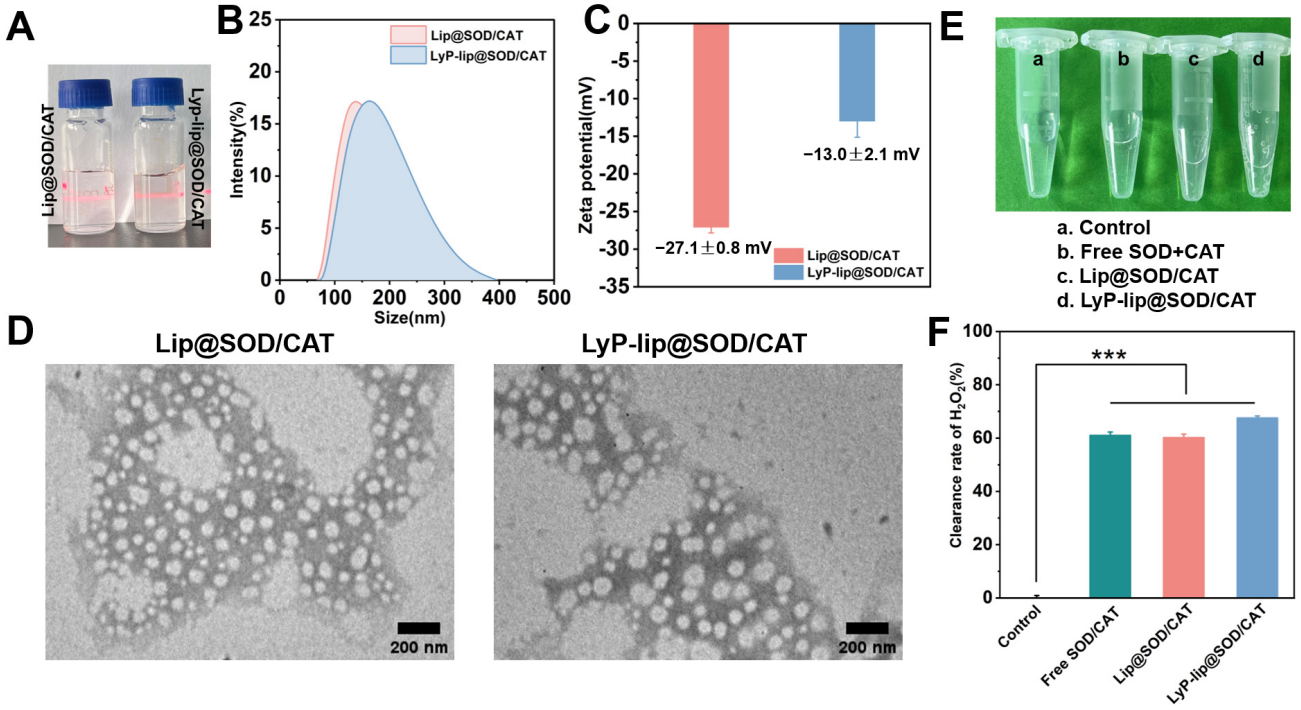

Fig. 2. Characterization and cytotoxicity of LyP-lip@SOD/CAT. (A) The Tyndall effect of Lip@SOD/CAT and LyP-lip@SOD/CAT. The average size (B) and Zeta potential (C) of Lip@SOD/CAT and LyP-lip@SOD/CAT. (D) Transmission electron microscopy (TEM) images of Lip@SOD/CAT and LyP-lip@SOD/CAT. (E) Photograph showing the O_2 production of different samples in hydrogen peroxide (H_2O_2) solutions. a. Control (50mM H_2O_2 without SOD or CAT), b. 50mM H_2O_2 with Free SOD+CAT, c. 50mM H_2O_2 with Lip@SOD/CAT, d. 50mM H_2O_2 with LyP-lip@SOD/CAT. (F) The H_2O_2 scavenging efficiency of different samples. ***$p < 0.001$, n = 3.

Results

Preparation and Characterization of LyP-lip@SOD/CAT

Fig. 1 illustrates the procedural steps involved in the synthesis of liposomes. DOTAP, a cationic lipid material, interacts with negatively charged SOD or CAT molecules through electrostatic interactions. The extraction of SOD and CAT from the aqueous phase to the organic phase using DOTAP was carried out based on the Bligh and Dyer monophase method [22]. The binding efficiencies of DOTAP to SOD and CAT were quantified using fluorescence quantitation, resulting in 99.0 ± 1.4% and 73.0 ± 1.7%, respectively (refer to **Supplementary Fig. 1**). These results demonstrated the successful extraction of antioxidant enzymes into the organic phase using DOTAP. This phase was subsequently mixed with other lipid materials to create liposomes employing the film dispersion method. The encapsulation rates of SOD and CAT within the liposomes were determined to be 56.78 ± 1.14% and 63.24 ± 1.02%, respectively (see **Supplementary Fig. 2**). This highlighted that the liposomes produced by this method can encapsulate two macromolecular proteases simultaneously. Measurements of the hydrodynamic diameters revealed values of 167.1 ± 10.8 nm for Lip@SOD/CAT and 159.5 ± 2.6 nm for LyP-lip@SOD/CAT, each possessing a polydispersity index (PDI) of 0.211 ± 0.040 and 0.208 ± 0.056, respectively, as depicted in Fig. 2B. Moreover, the aqueous solutions of the liposomes exhibited a distinct Tyndall effect, as shown in Fig. 2A. The Zeta potential of LyP-lip@SOD/CAT shifted from –27.1 ± 0.8 mV (for Lip@SOD/CAT) to –13.0 ± 2.1 mV, signifying successful attachment of the LyP-1 peptide to the liposome surface (see Fig. 2C). TEM characterization (Fig. 2D) displayed spherical and uniformly dispersed morphology for both Lip@SOD/CAT and LyP-lip@SOD/CAT nanoparticles. Studies report that nanoparticles within the size range of 10 to 200 nm, possessing negative electronegativity, exhibited prolonged circulation times *in vivo*, reduced macrophage uptake, and enhanced accumulation in AS lesion areas [23]. Therefore, nanoparticles prepared through this method are anticipated to achieve extended circulation *in vivo*, enabling effective accumulation within AS lesion areas.

The natural catalase exhibits a potent catalytic effect in decomposing hydrogen peroxide into water and oxygen [24]. To confirm the catalytic activity of encapsulated CAT, the clearance of H_2O_2 was assessed. The control aqueous solution lacked H_2O_2 scavenging ability. Notably, evident bubbles were observed within five minutes of reaction

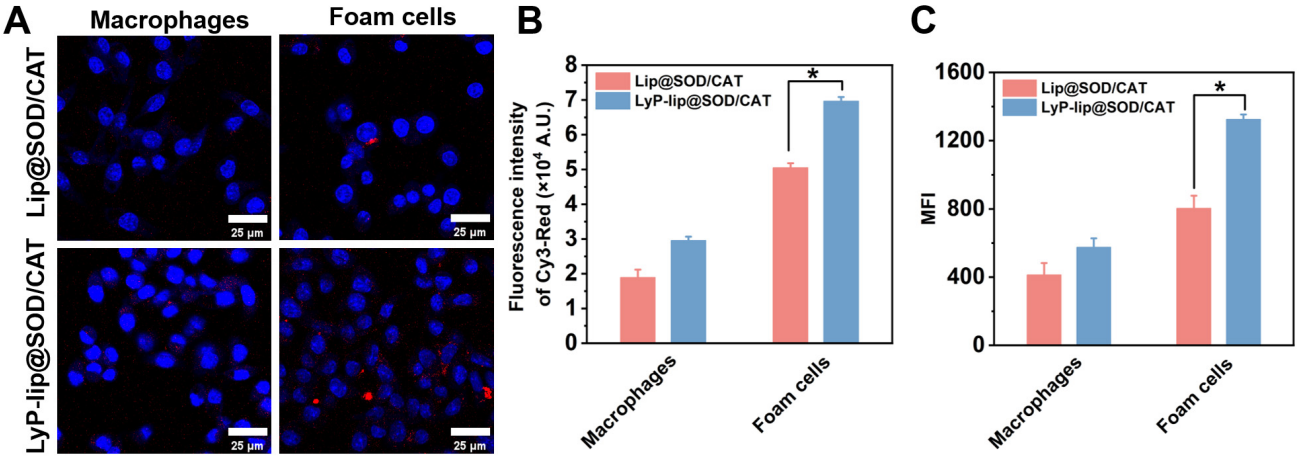

Fig. 3. Preferential association of LyP-lip@SOD/CAT to foam cells *in vitro*. (A) Cellular uptake of Lip@SOD/CAT and LyP-lip@SOD/CAT by CLSM. The nucleus was stained with Hoechst 33342 (blue). The Lip@SOD/CAT and LyP-lip@SOD/CAT were labeled with Cy3 (red). (B) Quantification of Cy3 red fluorescence intensity based on (A) by ImageJ (ImageJ2, National Institutes of Health, Bethesda, MD, United States). (C) Mean fluorescence intensity of the cells by flow cytometry. *$p < 0.05$, n = 3.

time for the free SOD and CAT, Lip@SOD/CAT, and LyP-lip@SOD/CAT groups (refer to Fig. 2E). The clearance rates of H_2O_2 for the free SOD and CAT, Lip@SOD/CAT, and LyP-lip@SOD/CAT groups were determined as 61.2 $\pm$ 1.1%, 60.3 $\pm$ 1.2%, and 67.7 $\pm$ 0.6%, respectively (see Fig. 2F). These findings validated that the enzyme activity remains unaffected during the liposome preparation process.

Targeting effect of LyP-lip@SOD/CAT to Foam Cells In Vitro

It has been documented that the cyclic peptide LyP-1 demonstrates exceptional penetration into atherosclerotic plaques by binding to p32, a protein often overexpressed in inflammatory cells like foam cells [25]. The evaluation of LyP-1-modified liposomes' affinity for both normal macrophages and foam cells was conducted using laser confocal microscopy. Hoechst 33342 was applied to stain the nucleus of the cells to indicate the location of cells, and the Cy3 fluorescent molecular was labeled on both Lip@SOD/CAT and LyP-1-lip@SOD/CAT to investigate the uptake behavior of the two liposomes for both normal macrophages and foam cells. As seen in Fig. 3A, for normal macrophages the Cy3 fluorescence was weak in both Lip@SOD/CAT and LyP-1-lip@SOD/CAT treated groups. For foam cells, the Cy3 fluorescence in both the two liposome treated groups was increased, with the LyP-1-lip@SOD/CAT treated foam cells having the strongest Cy3 fluorescence in the four experimental groups. These results indicated no discernible difference in uptake efficiency between normal macrophages for liposomes, irrespective of LyP-1 modification. However, when macrophages were induced to develop into foam cells, the uptake of both Lip@SOD/CAT and LyP-lip@SOD/CAT increased (Fig. 3A,B). Furthermore, in the case of foam cells, the uptake of LyP-lip@SOD/CAT demonstrated a significantly higher efficiency compared to that of Lip@SOD/CAT (Fig. 3C). This particular property signifies the effectiveness of LyP-lip@SOD/CAT in specifically targeting foam cells within AS plaques, thereby facilitating antioxidant effects.

Antioxidant and Anti-Inflammatory Effects of LyP-lip@SOD/CAT In Vitro

Recognized as a crucial small molecule, ROS plays a pivotal role in regulating diverse cellular and biological processes, and its excessive accumulation can trigger vascular damage [26]. Given the ROS scavenging activity associated with SOD and CAT, the antioxidant and anti-inflammatory effects of LyP-lip@SOD/CAT were investigated. DCFH-DA, a fluorescent probe sensitive to ROS, was utilized to assess ROS levels within cells. As depicted in Fig. 4A, the fluorescence intensity in the positive control group treated with LSP notably increased in comparison to the negative control group. Moreover, the free SOD and CAT-treated group exhibited a robust fluorescence intensity, indicative of a limited antioxidant effect by the free proteases. Conversely, the fluorescence intensities observed in the Lip@SOD/CAT and LyP-lip@SOD/CAT groups markedly decreased to lower levels, with LyP-lip@SOD/CAT demonstrating an even further reduction. These findings suggest that LyP-lip@SOD/CAT potentially enhances the antioxidant effects of SOD and CAT by facilitating increased cellular uptake of the drugs.

IL-1β, MCP-1, and TNF-α are recognized as proatherogenic inflammatory factors and play significant roles in all stages of AS, from initial endothelial dysfunction to the subsequent formation and destabilization of plaques [27]. To explore the *in vitro* anti-inflammatory properties of LyP-lip@SOD/CAT, the levels of typical inflammatory cy-

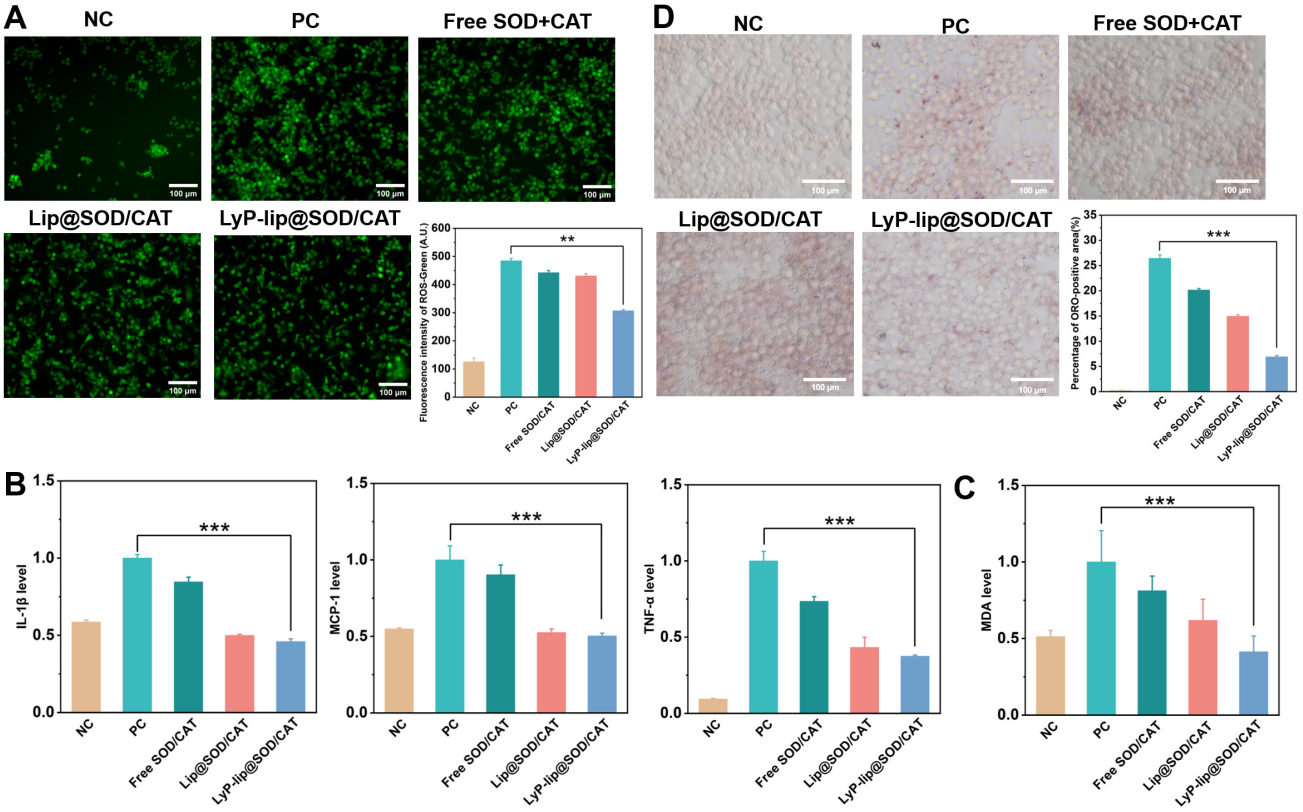

Fig. 4. Antioxidant, anti-inflammatory and promoting lipid efflux mechanism *in vitro*. (A) Detection of 2′,7′-Dichlorodihydrofluorescein diacetate (DCFH-DA) reactive oxygen species in cells, and quantification of DCFH-DA green fluorescence intensity by ImageJ. (B) The levels of typical inflammatory cytokines such as interleukin-1β (IL-1β), monocyte chemoattractant protein-1 (MCP-1), and tumor necrosis factor-α (TNF-α) by enzyme-linked immunosorbent assay (ELISA). (C) Intracellular lipid oxidation levels by malonaldehyde (MDA) assay. (D) Oil Red O (ORO) staining pictures of cellular lipids, and quantitation of ORO-positive area (red area) in cell staining by ImageJ. $^{**}p < 0.01$, $^{***}p < 0.001$, n = 3.

tokines (IL-1β, MCP-1, and TNF-α) were quantified using ELISA. In the positive control group, macrophages treated with LPS exhibited significantly elevated secretion of inflammatory factors, with IL-1β and MCP-1 levels doubling, and TNF-α levels increasing nearly tenfold. The free proteases demonstrated limited efficacy in reducing the secretion of these inflammatory factors. Conversely, treatment with Lip@SOD/CAT and LyP-lip@SOD/CAT resulted in decreased levels of inflammatory factors compared to the positive control group. Specifically, in the Lip@SOD/CAT-treated group, IL-1β, MCP-1, and TNF-α levels were reduced to 50.0 $\pm$ 0.7%, 52.6 $\pm$ 2.3%, and 43.3 $\pm$ 6.7%, respectively, compared to the positive group. Moreover, the LyP-lip@SOD/CAT-treated group exhibited further reductions, with IL-1β, MCP-1, and TNF-α levels decreasing to 45.9 $\pm$ 1.8%, 50.3 $\pm$ 1.9%, and 37.4 $\pm$ 0.8%, respectively (Fig. 4B). These results indicate that LyP-lip@SOD/CAT effectively diminishes pro-atherosclerotic inflammatory factors *in vitro*, thereby potentially slowing down the progression of AS to a certain extent.

Anti-Lipid Oxidation and Lipid Efflux Promotion In Vitro

Ox-LDL concentration is a critical marker for AS risk and a primary therapeutic target for AS [28]. Macrophages avidly internalize Ox-LDL, accumulating lipids to form “foam cells”, contributing to lipid droplet accumulation. Ox-LDL diminishes macrophage migration, thus fostering lipid plaque formation [29]. A strategy to impede plaque formation involves inhibiting lipid oxidation while promoting macrophage lipid efflux. To investigate whether LyP-lip@SOD/CAT could hinder lipid oxidation, a MDA assay was conducted. Fig. 4C illustrates that after treatment with Lip@SOD/CAT and LyP-lip@SOD/CAT, cellular lipid oxidation levels reduced by 61.8 $\pm$ 13.8% and 41.3 $\pm$ 10.4%, respectively, compared to the positive control group. These findings suggest that the liposomes effectively mitigate lipid oxidation, with LyP-lip@SOD/CAT demonstrating an enhanced effect in inhibiting lipid oxidation by facilitating increased protease delivery into cells.

Furthermore, the lipid efflux promotion effect was assessed by inducing macrophages to develop into foam cells through stimulation with Ox-LDL, followed by stain-

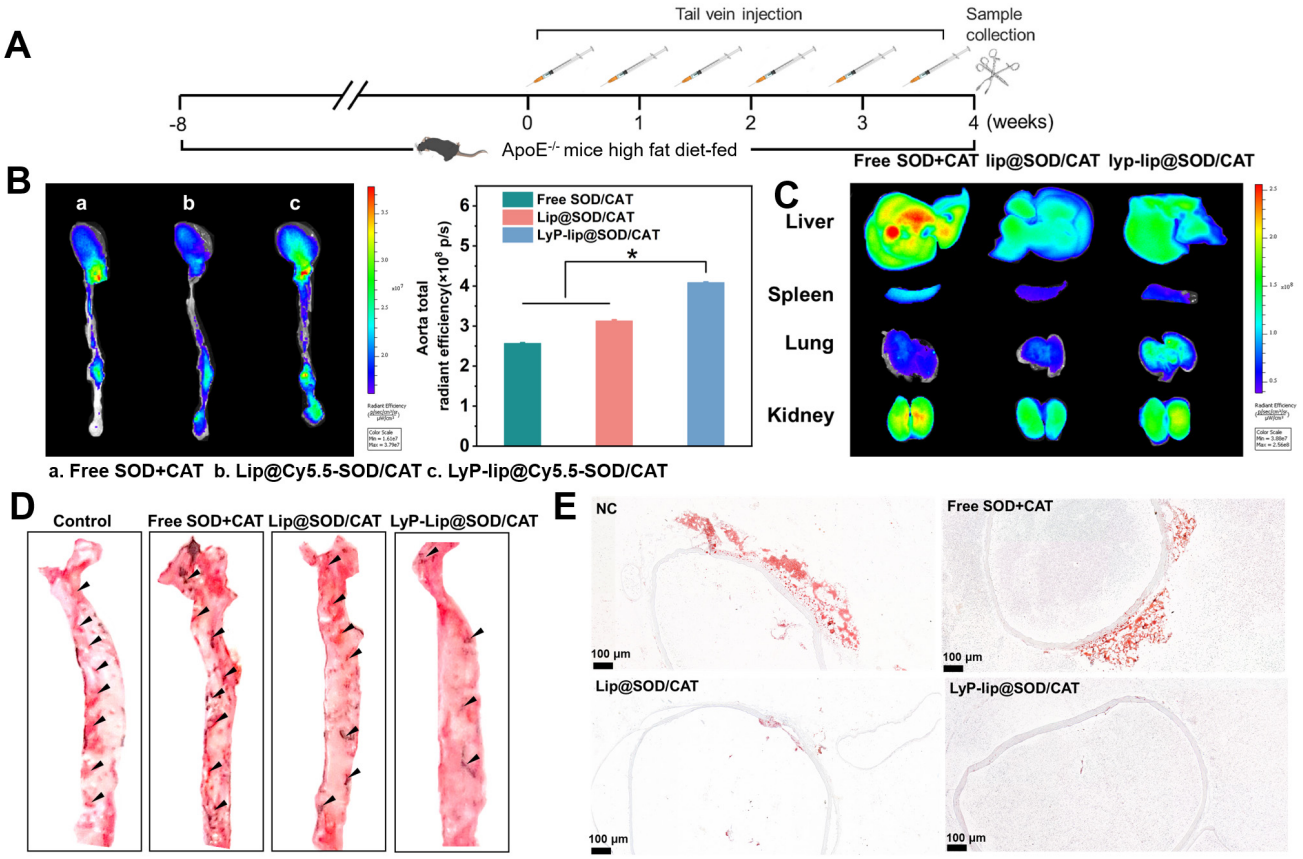

Fig. 5. Pharmacodynamic evaluation *in vivo*. (A) Establishment of atherosclerosis model in ApoE$^{-/-}$ mice. (B) *In vivo* representative images of Cy5.5 fluorescent signals in the aorta. a. Free SOD+CAT, b. Lip@Cy5.5-SOD/CAT, c. LyP-lip@Cy5.5-SOD/CAT. (C) *In vivo* representative images of Cy5.5 fluorescent signals in major organs (liver, spleen, lung, and kidney). (D) Oil Red O staining of whole aortas. Black arrows indicate ORO-positive areas. (E) ORO staining of the atherosclerotic plaques in aorta. *$p < 0.05$, n = 3.

ing with Oil Red O to evaluate lipid levels. Illustrated in Fig. 4D, distinct red spots were evident in the positive control group and the free drug group under bright field microscopy. In contrast, the Lip@SOD/CAT group displayed less conspicuous Oil Red O staining, and the staining intensity deepened notably upon treatment with LyP-Lip@SOD/CAT. This reinforced the notion of lipid metabolism promotion by LyP-Lip@SOD/CAT specifically for foam cells.

Plaque-Targeting Ability of LyP-lip@SOD/CAT in Vivo

The targeted effect of LyP-lip@SOD/CAT *in vivo* was demonstrated in an ApoE$^{-/-}$ mouse model of AS, established as outlined in Fig. 5A. Subsequent to 8 hours of drug administration, the hearts and aortas of the mice were isolated and examined using a fluorescence imaging system. As anticipated (depicted in Fig. 5B), LyP-lip@SOD/CAT exhibited a comparatively higher fluorescence signal in the aortic tree when compared to Lip@SOD/CAT, indicating a plausible plaque-targeting effect mediated by LyP-1 peptides.

Additionally, our observations revealed a reduced uptake of both Lip@SOD/CAT and LyP-lip@SOD/CAT in macrophage-rich scavenging organs, notably the spleen and liver, at 8 hours post-injection (Fig. 5C). This finding aligns with prior studies suggesting that nanoparticle functionalization through PEGylation could attenuate their clearance *in vivo* [30].

The Pro-Lipid Efflux Effect of LyP-lip@SOD/CAT in Vivo

The extent of lipid plaque accumulation serves as a crucial indicator of atherosclerosis treatment efficacy. Therefore, the aortas collected after 4 weeks of drug administration were stained using the ORO reagent to assess the plaque-reducing effect of LyP-lip@SOD/CAT (Fig. 5D). Significantly large ORO-positive areas were evident in the negative control and free drug groups, whereas a notable reduction in positive areas was observed in the Lip@SOD/CAT group. Moreover, the LyP-lip@SOD/CAT group exhibited the fewest ORO-positive areas, suggesting its capacity to diminish lipid plaques within the aorta in ApoE$^{-/-}$ mice, thus demonstrating an effective role in eliminating AS. Furthermore, the ORO staining results of

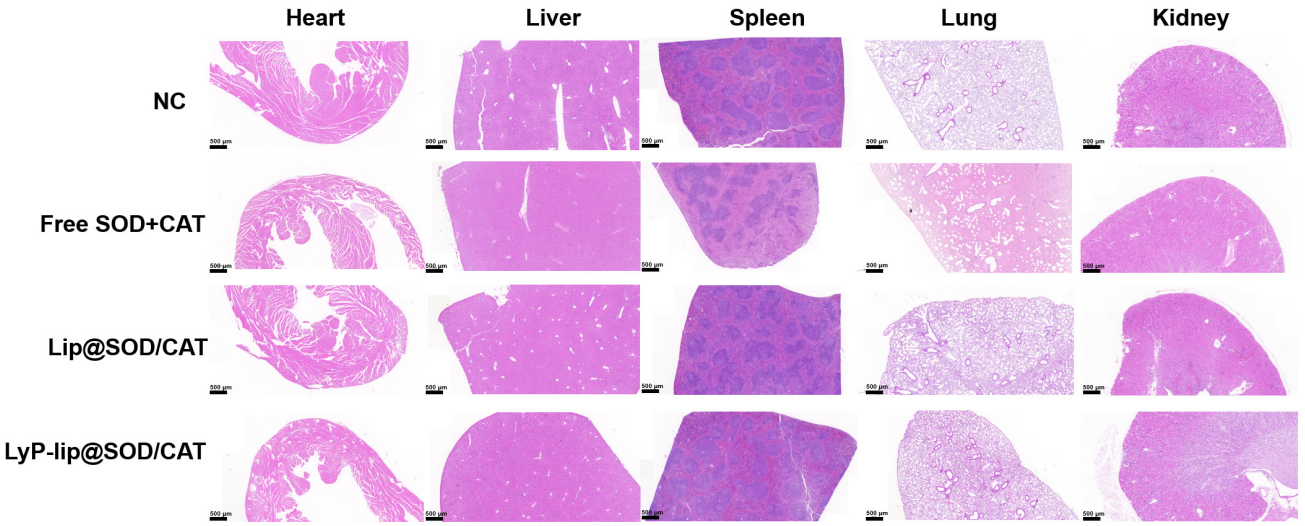

Fig. 6. Representative Hematoxylin and Eosin (H&E) staining images of the major organs.

the aortic sections provided additional evidence supporting the efficient lipid scavenging ability of LyP-lip@SOD/CAT (Fig. 5E).

Safety of LyP-lip@SOD/CAT In Vitro and Vivo

An MTT assay was conducted to demonstrate the lack of cytotoxicity associated with the liposomes (Lip@SOD/CAT and LyP-Lip@SOD/CAT) *in vitro* (**Supplementary Fig. 3**). Throughout the course of drug treatment, observation of the mice's body weight revealed no significant changes (**Supplementary Fig. 4**). Furthermore, histological examination of major organs using H&E staining was carried out to assess toxicity. As depicted in Fig. 6, no evident pathological abnormalities were observed in the normal organs (heart, liver, spleen, lung, and kidneys), indicating the commendable biocompatibility and biosafety profile of LyP-lip@SOD/CAT. Consequently, these results validate that LyP-lip@SOD/CAT effectively inhibits atherosclerosis-induced oxidative stress, exerting a plaque-reducing effect with anticipated high selectivity and satisfactory low toxicity.

Discussion

Anti-oxidative therapy has garnered attention as a promising approach in atherosclerosis treatment [3]. Enzymes, among various antioxidants, have been considered promising due to their specificity and minimal side effects. However, their instability both *in vitro* and *in vivo* has limited their effectiveness [13]. The liposome drug delivery system developed in this study aims to address these challenges encountered in enzyme delivery. Through an enhanced film hydration method, enzymes were initially incubated with cationic lipids to form protein-lipid complexes, enabling their encapsulation within the liposomes [31]. The obtained results including zeta potential (Fig. 2C), the encapsulation rates for SOD and CAT, and catalytic activity tests (Fig. 2E) of Lip@SOD/CAT corroborate the efficient protection provided by the prepared liposomes for the enzymes. This methodology demonstrates a promising strategy to overcome enzyme instability issues and enhance their delivery for potential therapeutic applications in atherosclerosis.

The utilization of nanomaterials has opened unprecedented avenues for AS treatment; however, the lack of effective targeting strategies remains a significant hurdle in the successful application of nanoparticles in AS therapy [32]. The cyclic peptide LyP-1, recognized for its binding affinity to p32 receptors expressed on foam cells [19], emerges as a potential target for atherosclerotic lesions. Our cellular uptake experiments validated the targeting effect of LyP-1 for foam cells (Fig. 3). Notably, while there was no substantial difference in the uptake of Lip@SOD/CAT and LyP-lip@SOD/CAT by macrophages, the cellular uptake of LyP-lip@SOD/CAT significantly increased when incubated with foam cells. Furthermore, the *in vivo* fluorescence imaging experiment indicated that LyP-lip@SOD/CAT could effectively target more enzymes to the AS plaque areas (Fig. 5B,C). Based on these findings, it is postulated that LyP-1 selectively binds to specific molecules expressed on foam cells, thereby directing the delivery of drugs specifically to these cells while sparing normal macrophages. This suggests that LyP-1 holds promise as a targeting peptide for AS-targeted drug delivery.

Given the remarkable enzyme protective capability and targeting efficiency of LyP-lip@SOD/CAT, we postulated that this engineered targeting delivery system could efficiently accumulate within AS regions, thereby exerting an antioxidant effect to eliminate established AS lipid plaques. *In vitro* antioxidant assays substantiated that LyP-lip@SOD/CAT retained potent antioxidant activity, both

at the solution level (Fig. 2E,F) and within cellular environments (Fig. 4A), even when enclosed within liposomes. Oxidative stress is widely acknowledged to activate various transcription factors involved in inflammatory pathways. Inflammation triggered by oxidative stress is a primary contributor to chronic diseases like AS [33]. Moreover, our experiments evaluating the anti-inflammatory properties of LyP-lip@SOD/CAT demonstrated that liposomes loaded with antioxidant enzymes were effective in mitigating the inflammatory state. This was evidenced by a reduced release of inflammatory factors (IL-1β, MCP-1, and TNF-α) from inflammatory macrophages (Fig. 4B). These findings further underscored the potential of LyP-lip@SOD/CAT in attenuating oxidative stress-induced inflammation, signifying its promising role in addressing chronic diseases like AS.

Elevated levels of ROS can stimulate the transformation of low-density lipoprotein (LDL) into Ox-LDL, triggering the formation of foam cells, a prominent characteristic of atherosclerotic lesions [3]. In our research, we examined the impact of LyP-lip@SOD/CAT on foam cell formation to assess the potential AS treatment effect of the developed drug delivery system. As demonstrated by lipid metabolism experiments conducted both *in vitro* (Fig. 4D) and *in vivo* (Fig. 5D,E), LyP-lip@SOD/CAT exhibited the ability to enhance the lipid efflux from macrophages while reducing lipid accumulation within atherosclerotic plaques. This effect could potentially contribute to the restoration of diseased atherosclerotic vessels. Furthermore, our investigation confirmed the safety profile of LyP-lip@SOD/CAT (Fig. 6), highlighting its potential as a reliable protein drug delivery vector and an effective AS-targeted drug delivery system. These findings collectively positioned LyP-lip@SOD/CAT as a promising candidate for AS treatment owing to its capacity to counteract foam cell formation and its demonstrated safety as a drug delivery system.

Conclusions

In summary, LyP-lip@SOD/CAT showcases promising attributes including its ability to target atherosclerotic plaques, efficiently scavenge excess ROS, curb oxidative stress, and facilitate macrophage lipid efflux at plaque sites. This study emphasizes the potential of LyP-lip@SOD/CAT as a straightforward yet promising nano reagent for antioxidant-based treatment of atherosclerosis.

Availability of Data and Materials

The data used to support the findings of this study are available from the corresponding author upon request.

Author Contributions

SZ: conceptualization, writing—original draft, writing—review and editing, methodology, supervision; DL: investigation, methodology, writing—original draft, writing—revising; CC: conceptualization, writing—review and editing, supervision; JZ: data curation, investigation, writing—original draft; SL: software, formal analysis, writing—revising; RS: methodology, data curation, writing—revising; RH: methodology, investigation, writing—revising. All authors gave final approval of the version to be published and agreed to be accountable for all aspects of the work.

Ethics Approval and Consent to Participate

All mouse experiments were performed in accordance with the applicable guidelines and regulations approved by the Animal Experimentation and Laboratory Animal Welfare Committee of Capital Medical University (AEEI-2023-027).

Acknowledgment

The authors gratefully acknowledge the support from Beijing Area Major Laboratory of Peptide and Small Molecular Drugs, Engineering Research Center of Endogenous Prophylactic of Ministry of Education of China, and Beijing Laboratory of Biomedical Materials.

Funding

This work was supported by the National Natural Science Foundation (81502688), Beijing Natural Science Foundation Program and Scientific Research Key Program of Beijing Municipal Commission of Education (KM201810025019), and a basic-clinical key research grant (16JL72, 17JL67) from Capital Medical University, the Importation and Development of High-Caliber Talents Project of Beijing Municipal Institutions (2013–2015), R&D Program of Beijing Municipal Education Commission (KM202210025024).

Conflict of Interest

The authors declare no conflict of interest.

Supplementary Material

Supplementary material associated with this article can be found, in the online version, at https://doi.org/10.24976/Discov.Med.202436181.32.

References

[1] Roth GA, Mensah GA, Johnson CO, Addolorato G, Ammirati E, Baddour LM, *et al*. Global Burden of Cardiovascular Diseases and Risk Factors, 1990-2019: Update From the GBD 2019 Study. Journal of the American College of Cardiology. 2020; 76: 2982–3021.

[2] Libby P, Buring JE, Badimon L, Hansson GK, Deanfield J, Bit-

tencourt MS, *et al*. Atherosclerosis. Nature Reviews. Disease Primers. 2019; 5: 56.

[3] Wang Y, Li L, Zhao W, Dou Y, An H, Tao H, *et al*. Targeted Therapy of Atherosclerosis by a Broad-Spectrum Reactive Oxygen Species Scavenging Nanoparticle with Intrinsic Anti-inflammatory Activity. ACS Nano. 2018; 12: 8943–8960.

[4] Malekmohammad K, Sewell RDE, Rafieian-Kopaei M. Antioxidants and Atherosclerosis: Mechanistic Aspects. Biomolecules. 2019; 9: 301.

[5] Andrews NP, Prasad A, Quyyumi AA. N-acetylcysteine improves coronary and peripheral vascular function. Journal of the American College of Cardiology. 2001; 37: 117–123.

[6] Goszcz K, Deakin SJ, Duthie GG, Stewart D, Leslie SJ, Megson IL. Antioxidants in Cardiovascular Therapy: Panacea or False Hope? Frontiers in Cardiovascular Medicine. 2015; 2: 29.

[7] Wang Y, Branicky R, Noë A, Hekimi S. Superoxide dismutases: Dual roles in controlling ROS damage and regulating ROS signaling. The Journal of Cell Biology. 2018; 217: 1915–1928.

[8] Forman HJ, Zhang H. Targeting oxidative stress in disease: promise and limitations of antioxidant therapy. Nature Reviews. Drug Discovery. 2021; 20: 689–709.

[9] Pudlarz AM, Czechowska E, S Karbownik M, Ranoszek-Soliwoda K, Tomaszewska E, Celichowski G, *et al*. The effect of immobilized antioxidant enzymes on the oxidative stress in UV-irradiated rat skin. Nanomedicine (London, England). 2020; 15: 23–39.

[10] Kirkman HN, Gaetani GF. Mammalian catalase: a venerable enzyme with new mysteries. Trends in Biochemical Sciences. 2007; 32: 44–50.

[11] Gao X, Ma Y, Zhang G, Tang F, Zhang J, Cao J, *et al*. Targeted elimination of intracellular reactive oxygen species using nanoparticle-like chitosan- superoxide dismutase conjugate for treatment of monoiodoacetate-induced osteoarthritis. International Journal of Pharmaceutics. 2020; 590: 119947.

[12] Chen W, Schilperoort M, Cao Y, Shi J, Tabas I, Tao W. Macrophage-targeted nanomedicine for the diagnosis and treatment of atherosclerosis. Nature Reviews. Cardiology. 2022; 19: 228–249.

[13] Zeng Z, He X, Li C, Lin S, Chen H, Liu L, *et al*. Oral delivery of antioxidant enzymes for effective treatment of inflammatory disease. Biomaterials. 2021; 271: 120753.

[14] Kiaie N, Gorabi AM, Penson PE, Watts G, Johnston TP, Banach M, *et al*. A new approach to the diagnosis and treatment of atherosclerosis: the era of the liposome. Drug Discovery Today. 2020; 25: 58–72.

[15] Zuris JA, Thompson DB, Shu Y, Guilinger JP, Bessen JL, Hu JH, *et al*. Cationic lipid-mediated delivery of proteins enables efficient protein-based genome editing in vitro and in vivo. Nature Biotechnology. 2015; 33: 73–80.

[16] Koide H, Ochiai H, Suzuki H, Hirata S, Watanabe M, Yonezawa S, *et al*. Easy preparation of a liposome-mediated protein delivery system by freeze-thawing a liposome-protein complex. Journal of Materials Chemistry. B. 2022; 10: 6768–6776.

[17] Song N, Zhao L, Zhu M, Zhao J. Recent progress in LyP-1-based strategies for targeted imaging and therapy. Drug Delivery. 2019; 26: 363–375.

[18] She ZG, Hamzah J, Kotamraju VR, Pang HB, Jansen S, Ruoslahti E. Plaque-penetrating peptide inhibits development of hypoxic atherosclerotic plaque. Journal of Controlled Release: Official Journal of the Controlled Release Society. 2016; 238: 212–220.

[19] Benne N, Martins Cardoso R, Boyle AL, Kros A, Jiskoot W, Kuiper J, *et al*. Complement Receptor Targeted Liposomes Encapsulating the Liver X Receptor Agonist GW3965 Accumulate in and Stabilize Atherosclerotic Plaques. Advanced Healthcare Materials. 2020; 9: e2000043.

[20] Marqués-Gallego P, de Kroon AIPM. Ligation strategies for targeting liposomal nanocarriers. BioMed Research International. 2014; 2014: 129458.

[21] Li J, Lin S, Vanhoutte PM, Woo CW, Xu A. Akkermansia Muciniphila Protects Against Atherosclerosis by Preventing Metabolic Endotoxemia-Induced Inflammation in Apoe-/- Mice. Circulation. 2016; 133: 2434–2446.

[22] BLIGH EG, DYER WJ. A rapid method of total lipid extraction and purification. Canadian Journal of Biochemistry and Physiology. 1959; 37: 911–917.

[23] Peters EB, Kibbe MR. Nanomaterials to Resolve Atherosclerosis. ACS Biomaterials Science & Engineering. 2020; 6: 3693–3712.

[24] Sepasi Tehrani H, Moosavi-Movahedi AA. Catalase and its mysteries. Progress in Biophysics and Molecular Biology. 2018; 140: 5–12.

[25] Hamzah J, Kotamraju VR, Seo JW, Agemy L, Fogal V, Mahakian LM, *et al*. Specific penetration and accumulation of a homing peptide within atherosclerotic plaques of apolipoprotein E-deficient mice. Proceedings of the National Academy of Sciences of the United States of America. 2011; 108: 7154–7159.

[26] Kattoor AJ, Pothineni NVK, Palagiri D, Mehta JL. Oxidative Stress in Atherosclerosis. Current Atherosclerosis Reports. 2017; 19: 42.

[27] Tousoulis D, Oikonomou E, Economou EK, Crea F, Kaski JC. Inflammatory cytokines in atherosclerosis: current therapeutic approaches. European Heart Journal. 2016; 37: 1723–1732.

[28] Halasz G, Piepoli MF. Focus on Atherosclerosis and Lipids. European Journal of Preventive Cardiology. 2021; 28: 799–802.

[29] Wang D, Yang Y, Lei Y, Tzvetkov NT, Liu X, Yeung AWK, *et al*. Targeting Foam Cell Formation in Atherosclerosis: Therapeutic Potential of Natural Products. Pharmacological Reviews. 2019; 71: 596–670.

[30] Liu M, Li J, Zhao D, Yan N, Zhang H, Liu M, *et al*. Branched PEG-modification: A new strategy for nanocarriers to evade of the accelerated blood clearance phenomenon and enhance antitumor efficacy. Biomaterials. 2022; 283: 121415.

[31] Kheirolomoom A, Kim CW, Seo JW, Kumar S, Son DJ, Gagnon MKJ, *et al*. Multifunctional Nanoparticles Facilitate Molecular Targeting and miRNA Delivery to Inhibit Atherosclerosis in ApoE(-/-) Mice. ACS Nano. 2015; 9: 8885–8897.

[32] Xiao Z, Li Y, Xiong L, Liao J, Gao Y, Luo Y, *et al*. Recent Advances in Anti-Atherosclerosis and Potential Therapeutic Targets for Nanomaterial-Derived Drug Formulations. Advanced Science (Weinheim, Baden-Wurttemberg, Germany). 2023; 10: e2302918.

[33] Hussain T, Tan B, Yin Y, Blachier F, Tossou MCB, Rahu N. Oxidative Stress and Inflammation: What Polyphenols Can Do for Us? Oxidative Medicine and Cellular Longevity. 2016; 2016: 7432797.